RSC Advances

ROYAL SOCIETY OF CHEMISTRY

www.rsc.org/advances

$^{64}CuCl_2$ Produced by Direct Neutron Activation Route as a Cost-Effective Probe for Cancer Imaging: The Journey has Begun

Rubel Chakravarty,[1,#] Sudipta Chakraborty,[1,#] K. V. Vimalnath,[1] Priyalata Shetty,[1] Haladhar Dev Sarma,[2] P. A. Hassan[3] and Ashutosh Dash[1,*]*

[1]Isotope Production and Applications Division, [2]Radiation Biology and Health Sciences Division, [3]Chemistry Division, Bhabha Atomic Research Centre, Trombay, Mumbai 400 085, India

[#]*The authors contributed equally*

To whom all correspondences should be addressed:
Ashutosh Dash, Ph.D.
E-Mail: adash@barc.gov.in
Or
Rubel Chakravarty, Ph.D.
E-Mail: rubelc@barc.gov.in

ABSTRACT

Copper-64 ($t_{½}$ = 12.7 h., E.C. 45%, β^- 37.1%, β^+ 17.9%) is a promising radionuclide for positron emission tomography (PET) imaging which is generally produced by ^{64}Ni (p, n) ^{64}Cu reaction in a cyclotron. Despite excellent attributes of ^{64}Cu for PET imaging, the utility of this radioisotope is still limited to countries having good cyclotron facilities and excellent production logistics. We have explored the feasibility of using ^{64}Cu in the form of $^{64}CuCl_2$, produced in research reactors by (n, γ) route, as a probe for tumor imaging by PET. The production strategy has been optimized to obtain $^{64}CuCl_2$ with adequate specific activity and radionuclidic purity suitable for clinical use. Exploring copper metabolism as an imaging biomarker, $^{64}CuCl_2$ can directly be used as an effective probe for non-invasive visualization of tumors. The stability of $^{64}CuCl_2$ under physiological conditions was assessed by detailed *in vitro* studies in mouse serum medium. The biological efficacy of $^{64}CuCl_2$ was studied in C57BL/6 mice bearing melanoma tumors and Swiss mice bearing fibrosarcoma tumors. The results of the biodistribution studies revealed significant tumor uptake (7.64 ± 1.71 %ID/g in melanoma, 6.54 ± 1.41 %ID/g in fibrosarcoma) within 4 h post-injection, with good tumor-to-background contrast. To the best of our knowledge, this is the first study which employs neutron activated $^{64}CuCl_2$ as a potential radiotracer for PET imaging in preclinical settings. Owing to availability of several medium-flux nuclear reactors with good geographical distribution in different parts of the world, the promising results obtained in this study would set the stage for wide-scale utilization of neutron activated $^{64}CuCl_2$ as a cost-effective probe for PET imaging.

Keywords: $^{64}CuCl_2$, (n,γ)^{64}Cu, Cancer, Molecular imaging, PET, Radiotracer

INTRODUCTION

The role of molecular imaging to visualize, characterize, and quantify endogenous biological processes at the cellular and molecular levels in living subjects using a range of imaging modalities is well recognized.[1-4] Among various imaging modalities, PET is increasingly being used in clinics all over the world for medical decision making and patient management.[5] Evolution and continued success of PET, has been, in large part, due to the evolution of imaging technology and rapid development of specific probes using suitable positron-emitting radionuclides. The main factors contributing to the choice of the positron-emitting radionuclides are their physical and chemical characteristics, availability, and the timescale of the biological process intended to be studied.

Copper-64 ($t_{½}$ = 12.7 h., E.C. 45%, β^- 37.1%, β^+ 17.9%) is a unique intermediate half-lived positron-emitting radionuclide which decays by three processes, namely, electron capture, β^- and β^+ decays.[6] There appears to be enticing interest to consider the use of ^{64}Cu owing to simultaneous emission of β^- and β^+ particles, which holds promise not only in development of diagnostic radiotracers for PET imaging but can also be used in preparation of radiotherapeutic agents for cancer treatment.[7] While the attributes of ^{64}Cu is quite promising, utilization of this radioisotope is mostly limited to preclinical studies and that too mainly in the developed countries of the world.[7] Currently, use of ^{64}Ni (p, n) ^{64}Cu reaction in a cyclotron has remained as the most common procedure for the production of ^{64}Cu.[6] While this cyclotron production route constitutes a viable approach, the implicit need of cyclotron facilities and elaborate procedures of radiochemical separation and purification as well as excellent logistics for its supply to distant user sites are some of the issues that made availability of this radioisotope very limited. Competition from other established PET radiotracers based on ^{18}F and ^{68}Ga with easier

availability might be the other reason behind less popularity of this radioisotope in clinical context.

Copper-64 can also be produced in a nuclear reactor adopting thermal neutron capture, ^{63}Cu (n, γ) ^{64}Cu, or the fast neutron capture, ^{64}Zn (n, p) ^{64}Cu reactions.[8, 9] Though the latter route results in production of ^{64}Cu in a no-carrier-added (NCA) form, it requires access to the reactor with reasonably high fast neutron flux positions which is not available in majority of research reactor facilities across the world. On the other hand, majority of the radioisotopes produced in the research reactors across the world are the products of thermal neutron induced nuclear reactions, mainly by (n, γ) reaction.[10] Among the available options for production of ^{64}Cu, the ^{63}Cu (n, γ) ^{64}Cu reaction represents the least intricate route since it precludes the separation of ^{64}Cu from its precursor. Moreover, the neutron activation route involves negligible radioactive waste generation and is inexpensive.

While the ^{63}Cu (n, γ) ^{64}Cu production route is quite promising, this approach provides ^{64}Cu of low specific activity which is unsuitable for labeling receptor targeted ligands.[6, 7] In this premise, use of neutron activated ^{64}Cu in the form of $^{64}CuCl_2$ as a radiotracer for non-invasive assessment of various types of cancers was deemed worthy of consideration and there are few reports to support its merit.[11-14] It is worthwhile to point out that adaptation of this strategy would obviate the radiolabeling step, preclude the need of expensive target specific ligands such as peptides and antibodies, and would be easy to implement under current good manufacturing practices (cGMP) compliant conditions because simple target dissolution capabilities would suffice to produce the radiotracer in a form suitable for use in PET imaging.

Herein, we report a systematic approach for establishing $^{64}CuCl_2$ produced by direct neutron activation route in a medium flux research reactor as a cost-effective probe for cancer

imaging by PET. Towards this, the irradiation parameters (neutron flux and irradiation time) for production of $^{64}CuCl_2$ with adequate specific activity and radionuclidic purity for use as a PET radiotracer were optimized by theoretical calculations. The practicality of the approach was demonstrated by production of this radioisotope in several batches in the Dhruva reactor of our research centre. As a proof of concept, the efficacy of the radiotracer was established by biodistribution studies in C57BL/6 mice bearing melanoma tumors and Swiss mice bearing fibrosarcoma tumors.

EXPERIMENTAL

Materials and Equipment

Copper oxide (spectroscopic grade > 99.99 % pure) used as the target material for production of ^{64}Cu was obtained from E. Merck, Germany. All other chemicals were of Analytical Reagents (AR) grade and purchased from established manufacturers. Standard source of ^{152}Eu ($t_{½}$ = 13.6 y) was obtained from Amersham, Inc., USA. Flexible silica plates (coating thickness 0.25 mm) from J. T. Baker Chemical Company, USA were used for thin layer chromatography (TLC) studies. The activity of ^{64}Cu was measured using a pre-calibrated Capintec dose calibrator (Ramsey, NJ). The presence of radionuclidic impurities in ^{64}Cu was determined by recording gamma ray spectra using a calibrated high purity germanium detector (HPGe) detector coupled to a 4K multichannel analyzer (MCA) system. All other radioactivity measurements were carried out using a well-type NaI (Tl) scintillation counter, unless mentioned otherwise, keeping the baseline at 400 keV and a window of 200 keV thereby utilizing the 511 keV gamma photon of ^{64}Cu due to positron-annihilation. Dynamic light scattering (DLS)

measurements were performed using a Malvern 4800 Autosizer employing a 7132 digital correlator for the determination of hydrodynamic diameter.

Production of ^{64}Cu via (n, γ) Route

Copper-64 was produced by thermal neutron bombardment on natural CuO (69.1 % in ^{63}Cu) target. A known amount of target was taken in a quartz ampoule. After placing inside aluminum can, the ampoule was subsequently flame sealed and irradiated at a thermal neutron flux of ~ 1×10^{14} n.cm^{-2}.s^{-1} for 7 days in Dhruva research reactor at Bhabha Atomic Research Centre, India. At the end of irradiation, the irradiated targets were cooled for 24 h and subsequently dissolved in 5 mL of 1 M suprapure HCl by gentle warming inside a lead shielded facility. The resultant solution was evaporated to near dryness and reconstituted in 2 mL of de-ionized water.

Determination of Yield and Specific Activity of ^{64}Cu Produced via (n, γ) Route

After radiochemical processing, the activity of ^{64}Cu was measured using a dose calibrator. The activity of ^{64}Cu was accurately determined using HPGe detector coupled to MCA system. For this purpose, a small aliquot of ^{64}Cu was withdrawn and the γ-spectrum was recorded after appropriate dilution of the radioactivity so that the dead time of the detector was < 5 %. Energy and efficiency calibrations of the HPGe detector were carried out using standard ^{152}Eu reference source prior to the measurement of activity. The specific activity was determined from the total yield of ^{64}Cu and expressed as TBq/g of Cu.

Quality Control of ^{64}Cu Produced via (n, γ) Route

Radionuclidic Purity: The presence of radionuclidic impurities in ^{64}Cu produced via (n, γ) route could be determined from the γ-spectrum of ^{64}Cu recorded using HPGe detector coupled to MCA system, as described above. For accurate quantification of the level of radionuclidic impurities,

the γ-spectra of ^{64}Cu samples were recorded after allowing them to decay for 1 week. The characteristic γ-peaks corresponding to the extraneous radionuclides were monitored for determination of their radioactivity. From this data, the level of radionuclidic impurities in ^{64}Cu was calculated after proper decay corrections.

Radiochemical Purity: The radiochemical purity of ^{64}Cu produced in the form of $^{64}Cu^{2+}$ ions was determined by radio-thin layer chromatography (radio-TLC) assay. For this purpose, 5 µL of $^{64}CuCl_2$ solution was spotted on a TLC plate at 1.5 cm from the bottom. The chromatogram was developed in 0.1 M sodium citrate medium. Subsequently, the TLC plate was dried and cut into 1 cm pieces and activity of each piece was determined using a NaI (Tl) counter. The radiochemical purity of ^{64}Cu in the form of $^{64}Cu^{2+}$ ion was expressed as the percentage of the total activity which migrated to the solvent front (R_f = 0.9-1) in the chromatogram developed.

Determination of Octanol/Water Partition Coefficients (log D) of $^{64}CuCl_2$ and ^{64}Cu-NOTA Complex

The octanol/water partition coefficient (log D) of $^{64}CuCl_2$ was determined adopting the reported method. [15] In brief, 200 µL of $^{64}CuCl_2$ was added to 1.8 mL of phosphate buffered saline solution (pH ~ 7.4) and thoroughly mixed. Subsequently, 2 mL of 1-octanol was added to the above solution, vortexed for 1 - 2 min. The layers were separated by centrifugation and 100 µL aliquots were withdrawn from each layer and counted in a NaI(Tl) scintillation counter. A 0.8 mL aliquot of the octanol layer was withdrawn and added to an equal volume of normal saline solution and the extraction process was repeated, as above. The results of this back extraction were used to compute the ratio of the activity in octanol to phosphate buffered saline layers and the log D value was calculated.

Also, 1,4,7-triazacyclononane-1,4,7-triacetic acid (NOTA) was radiolabeled with ^{64}Cu as per the reported procedure [16] and log D value for ^{64}Cu-NOTA complex at pH ~ 7.4 was determined as described above.

Study on Protein Aggregation in Mouse Serum in Presence of Cu^{2+} Ions by Dynamic Light Scattering

DLS measurements were carried out for mouse serum samples containing varied amounts of $CuCl_2$ (6.7 – 33.3 μg Cu per mL) using a Malvern 4800 photon correlation spectrometer. The instrument is equipped with a He-Ne laser (λ = 632.8 nm) with a vertically polarized light. All measurements were carried out at an output power of 15 mW and at 25 ± 0.1 °C. The intensity correlation functions were first analyzed by the method of cumulants to extract the average hydrodynamic diameter and polydispersity index of size distribution. Since the polydispersity index was high (> 0.3) in all samples, all data were analyzed by the CONTIN algorithm for inverse Laplace transformation of the correlation function. The corresponding fits are shown as solid line in the graph. The correlation function was measured five times for each sample.

***In Vitro* Stability of $^{64}CuCl_2$ in Mouse Serum**

The stability of $CuCl_2$ in mouse serum medium was studied by low resolution nuclear magnetic resonance (NMR) diffusivity measurements using Xigo Nanotools Acorn Area instrument. The homogenous solution of $CuCl_2$ in mouse serum (20 μg Cu / mL of serum) was filled in the NMR tube and inserted into the magnetic field. The relaxation time was determined at 25 ± 0.1 °C by T_2 measurement using Carr-Purcell-Meiboom-Gill (CPMG) method.[17]

The stability $CuCl_2$ in mouse serum medium was also studied by radio-TLC assay. For this purpose, tracer level of ^{64}Cu was mixed with inactive $CuCl_2$ and added to mouse serum to maintain an effective concentration of 20 μg Cu / mL and incubated at 37 ± 0.1 °C. The radio-

TLC pattern was developed adopting the procedure described earlier. The stability of $CuCl_2$ in mouse serum over a prolonged period of time was analyzed by radio-TLC assays at different time intervals.

Biodistribution Studies in Tumor Bearing Mice

All animal studies were conducted under a protocol approved by the Bhabha Atomic Research Centre Animal Ethics Committee. The biological behavior of the radiotracer prepared was studied in C57BL/6 mice bearing melanoma tumors and Swiss mice bearing fibrosarcoma tumors. Melanoma tumors were developed by injecting ~ 1×10^6 melanoma cells (ATCC®-CRL-6475™) suspended in 200 µL of phosphate buffered saline (PBS) subcutaneously into the right thigh of each C57/BL6 mouse weighing 20 - 25 g. Similarly, fibrosarcoma tumors were raised in Swiss mice by injecting ~ 1×10^6 fibrosarcoma cells (ATCC® CRL-2295™) suspended in 200 µL of phosphate buffered saline (PBS) subcutaneously into the right thigh of each mouse weighing 20 - 25 g. The animals were observed for visibility of tumors and subsequently allowed to grow for about 2 weeks to attain a tumor mass of 0.2 - 0.4 g.

The radiotracer ($^{64}CuCl_2$ in 0.9 % NaCl medium, 100 µL, 3.7 – 5.5 MBq) was injected into each animal through a lateral tail vein. The animals were sacrificed by cardiac puncture post-anesthesia at 1, 4, 24 and 48 hours post-injection (p.i.). Four animals were used at each time point. Various organs, tissues, and tumors were excised after sacrifice, washed with physiological saline, dried, and the radioactivity associated with each organ and tissue was determined using a flat-type NaI(Tl) counter. The weight of each organ and tumor was also determined by using an analytical balance. The percent injected activity (%ID) in various organs, tissues, and tumor was calculated from the above data and expressed as percentage injected activity per gram (%ID/g) of organ/tissue.

As control experiment, ^{64}Cu-NOTA complex was prepared as per the reported procedure [16] and administered (100 μL, 3.7 – 5.5 MBq) in melanoma and fibrosarcoma tumor bearing mice and biodistribution studies were carried out as described above.

RESULTS

Production of ^{64}Cu via (n, γ) Route

Copper-64 can be produced by neutron activation of ^{63}Cu. The production of ^{64}Cu along with the possibility of formation of other radionuclidic impurities is indicated in **Figure 1**. During the course of irradiation, ^{64}Cu decays to stable ^{64}Zn by β^- decay, which in turn would undergo neutron activation to form long-lived ^{65}Zn ($t_{½}$ = 244 d) (**Figure 1A**). Also, ^{64}Cu decays by β^+ decay to stable ^{64}Ni, which would undergo neutron activation to form ^{65}Ni ($t_{½}$ = 2.5 h) (**Figure 1A**). Since, natural CuO is used for irradiation, ^{66}Cu ($t_{½}$ = 5.1 min) would also be produced by neutron activation of ^{65}Cu (**Figure 1A**). Apart from ^{65}Zn, other short lived radionuclidic impurities (^{65}Ni and ^{66}Cu) present in ^{64}Cu are not of much concern as they would decay completely within few hours after end of irradiation (**Figure 1B**).

The activity of ^{64}Cu produced by thermal neutron activation of natural CuO oxide in a research reactor can be theoretically calculated using the standard Bateman equations [18]:

$$N_{64Cu}(t) = N°_{63Cu}.\ \Lambda^*_{63Cu}\ \frac{\exp(-\Lambda_{63Cu}t) - \exp(-\Lambda_{64Cu}t)}{\Lambda_{64Cu} - \Lambda_{63Cu}} \quad \text{.....(1)}$$

$$A_{64Cu}(t) = N_{64Cu}(t) \times \lambda_{64Cu} \quad \text{.....(2)}$$

$$\Lambda^*_{63Cu} = \Lambda_{63Cu} = \sigma_{63Cu}\phi \quad \text{.....(3)}$$

$$\Lambda^*_{64Cu} = \Lambda_{64Cu} = \lambda_{64Cu} \quad \text{.....(4)}$$

where, N_{64Cu} (t) and A_{64Cu} (t) are the number of atoms and activity of ^{64}Cu produced on irradiation of ^{63}Cu target for time 't', σ_{63Cu} is the thermal neutron capture cross-section of ^{63}Cu, and λ_{64} is the decay constant of ^{64}Cu.

The yield of the extraneous radionuclide, ^{65}Zn, can also be calculated using similar Bateman equations:

$$N_{65Zn}(t) = N°_{63Cu}.\Lambda^{*}_{63Cu}.\Lambda^{*}_{64Cu}.\Lambda^{*}_{64Zn}\left\{\frac{\exp(-\Lambda_{63Cu}t)}{(\Lambda_{64Cu}-\Lambda_{63Cu})(\Lambda_{64Zn}-\Lambda_{63Cu})(\Lambda_{65Zn}-\Lambda_{63Cu})}+\frac{\exp(-\Lambda_{64Cu}t)}{(\Lambda_{63Cu}-\Lambda_{64Cu})(\Lambda_{64Zn}-\Lambda_{64Cu})(\Lambda_{65Zn}-\Lambda_{64Cu})}+\frac{\exp(-\Lambda_{64Zn}t)}{(\Lambda_{63Cu}-\Lambda_{64Zn})(\Lambda_{64Cu}-\Lambda_{64Zn})(\Lambda_{65Zn}-\Lambda_{64Zn})}+\frac{\exp(-\Lambda_{65Zn}t)}{(\Lambda_{63Cu}-\Lambda_{65Zn})(\Lambda_{64Cu}-\Lambda_{65Zn})(\Lambda_{64Zn}-\Lambda_{65Zn})}\right\} \quad \ldots\ldots(5)$$

$$A_{65Zn}(t) = N_{65Zn}(t) \times \lambda_{65Zn} \quad \ldots\ldots(6)$$

$$\Lambda^{*}_{64Zn} = \Lambda_{64Zn} = \sigma_{64Zn}\phi \quad \ldots\ldots(7)$$

$$\Lambda_{65Zn} = \lambda_{65Zn} \quad \ldots\ldots(8)$$

where, N_{65Zn} (t) and A_{65Zn} (t) are the number of atoms and activity of ^{65}Zn produced on irradiation of ^{63}Cu target for time 't', σ_{64Zn} is the thermal neutron capture cross-section of ^{64}Zn, and λ_{65} is the decay constant of ^{65}Zn.

Based on the above equations, activities of ^{64}Cu and ^{65}Zn produced during neutron irradiation of natural CuO at different neutron flux positions and for different irradiation times were theoretically calculated in order to arrive at the optimum conditions that would provide ^{64}Cu with maximal specific activity while ensuring that the contamination from ^{65}Zn impurity was negligibly low (**Figure 2**).

Figure 2A depicts the calculated specific activity of ^{64}Cu at different flux positions for different durations of irradiation. It is evident from the figure that the specific activity of ^{64}Cu generally increases with increase in flux of the irradiation position. However, the specific activity of ^{64}Cu reaches a level of saturation within 2 days of irradiation, indicating that this is the optimal irradiation time at all flux positions. When irradiation is carried out at flux $\leq 1 \times 10^{14}$ n.cm^{-2}.s^{-1}, the level of ^{65}Zn impurity formed in ^{64}Cu is negligibly low (**Figure 2B**). The level of the radionuclidic impurity significantly increases with increase in flux as well as the time of irradiation (**Figure 2A**).

Though, ^{64}Cu can be produced with appreciably high specific activity on irradiation at flux $> 1 \times 10^{14}$ n.cm^{-2}.s^{-1}, the radionuclidic impurity burden of long-lived ^{65}Zn is a cause of major concern from the perspective of clinical utility of this radioisotope. Owing to the short half-life of ^{64}Cu, the radionuclidic impurity burden of ^{65}Zn in ^{64}Cu would rapidly increase with time. Hence, in order to minimize the radionuclidic impurity in ^{64}Cu, it is essential to carry out the irradiation of ^{63}Cu under lower flux conditions ($\sim 1 \times 10^{14}$ n.cm^{-2}.s^{-1}). This would however lower the specific activity of ^{64}Cu (**Figure 2A**). A balance between specific activity and radionuclidic purity of ^{64}Cu would be required in order to utilize the radioisotope for clinical PET imaging.

Production Yield and Specific Activity of ^{64}Cu from Practical Irradiations via (n, γ) Route

The practicality of the theoretical calculations discussed in the previous section was experimentally demonstrated by production of ^{64}Cu by irradiation of natural CuO target in the Dhruva reactor at a flux of $\sim 1 \times 10^{14}$ n.cm^{-2}.s^{-1} for 7 days. Though the theoretical calculations indicated saturation of activity of ^{64}Cu on irradiation for > 2 d, the minimum time-slot for irradiation available in our research reactor is 7 days and the target cannot be taken out of the

reactor in between. On irradiation of 13 - 22 mg of natural CuO target, the activity of ^{64}Cu after radiochemical processing varied between 30 and 57 GBq, which is appreciably high for both preclinical as well as clinical studies (**Table 1**). The specific activity of ^{64}Cu produced via (n, γ) route in different batches was ~ 3 TBq/g. Owing to its simplicity, the production process is easily amenable for scale-up to meet the demand of the nuclear medicine community in future.

Quality Control of ^{64}Cu Produced via (n, γ) Route

Radionuclidic purity: The radionuclidic purity of ^{64}Cu produced was determined by γ-ray spectrometry using a calibrated HPGe detector coupled to MCA system (**Figure 1B**). The γ-ray spectra of ^{64}Cu recorded immediately after the radiochemical processing only shows the 511 keV annihilation peak and no photopeak corresponding to ^{65}Zn could be seen. However, when ^{64}Cu samples were decayed for 7 days, the 511 keV and 1115.5 keV photopeaks corresponding to ^{65}Zn could be seen in the γ-spectra (**Figure 1B**). Decay of ^{64}Cu samples for 7 days was required for quantitative estimation of the trace level of ^{65}Zn impurities, the characteristic photopeaks of which otherwise got masked by the intense 511 keV peak of ^{64}Cu in the γ-spectra. By analysis of the γ-spectra, the levels of radionuclidic impurities at end of radiochemical processing and 24 h after end of irradiation (as shown in **Table 1**) were calculated applying suitable decay corrections.

The level of ^{65}Zn present in ^{64}Cu was found to be < 10^{-5} % at the end other radiochemical processing (**Table 1**). Since radiochemical processing of ^{64}Cu was performed at least 8 h after the end of irradiation, the presence of other short-lived radioisotopes (^{65}Ni and ^{66}Cu) could not be detected. No other radionuclidic impurity in ^{64}Cu could be detected from the γ-spectra. Assuming that the radioisotope if approved for clinical studies would reach the hospitals only on the next day, the specific activity and radionuclidic purity of ^{64}Cu were determined at an interval

of 24 h after end of irradiation (**Table 1**). Though the specific activity decreased significantly within this period of time, the level of ^{65}Zn impurity was still negligibly low (< 10^{-5} %) and hence $^{64}CuCl_2$ was suitable for clinical use (**Table 1**). Irradiations were carried out in 5 different batches and the results were quite reproducible in all the batches.

Radiochemical Purity: For determination of radiochemical purity of ^{64}Cu, the TLC was developed in 0.1 M sodium citrate medium which would form copper citrate complex with ^{64}Cu in ionic form. On development of the chromatogram, the activity at the point of application (R_f = 0) indicates the presence of colloidal ^{64}Cu, while the activity at the solvent front (R_f = 0.9 – 1) is indicative of the amount of ^{64}Cu in ionic form (Cu^{2+}). After radiochemical processing, the radiochemical purity of ^{64}Cu in the form of Cu^{2+} ion was determined to be > 99 % in all the batches.

Determination of Octanol/Water Partition Coefficients (log D) of $^{64}CuCl_2$ and ^{64}Cu-NOTA Complex

The log D values of $^{64}CuCl_2$ and ^{64}Cu-NOTA at pH 7.4 (the physiological pH of blood serum) were determined to be – 2.5 ± 0.2 and – 2.2 ± 0.1 (n = 5), respectively, which indicates that both the compounds are highly hydrophilic in nature.

Study on Protein Aggregation in Mouse Serum in Presence of Cu^{2+} Ions by Dynamic Light Scattering

Serum albumin is an important protein present in blood and is capable of binding with various additives such as drugs, hormones, transition metal ions etc. [19] Reports indicate that the presence of metal ions such as Cu^{2+}, Zn^{2+} ions etc. lead to aggregation of a variety of proteins including human serum albumin. [19] To determine the cut-off limit for administration of neutron activated $^{64}CuCl_2$ in biological system so that aggregation of serum protein could be avoided,

varying amounts of $CuCl_2$ were added to mouse serum (6.7 – 33.3 μg Cu per mL) and characterized by DLS study. DLS is an ensemble averaged technique used to study the aggregation of proteins under different experimental conditions. As a control study, DLS measurement of 'blank' mouse serum medium was also recorded. DLS study of 'blank' mouse serum indicated presence of nanosized protein particles with effective hydrodynamic diameter ~76 nm. Particle size information after addition of varying amounts of $CuCl_2$ in mouse serum was obtained by analysis of the electric field correlation function, [g(τ)], calculated over a wide range of correlation time, τ.[20] A significant shift in g(τ) was observed only when the concentration of $CuCl_2$ in mouse serum was > 20 μg / mL, indicating the formation of colloidal aggregates above this concentration (**Figure 3A**). Moreover, the aggregation was found to be time dependant, once the concentration of Cu^{2+} ions exceeds 20 μg / mL. To understand the time-dependent increase in the particle size of the aggregates, DLS measurements were made at different time intervals after addition of $CuCl_2$ (26.7 μg Cu / mL) in mouse serum and g(τ) was calculated (**Figure 3B**). As indicated from the shift in g(τ), the effective particle size increased from 76 nm to 176 nm over a period of 40 min (inset of **Figure 3B**). This study indicated that in all *in vivo* studies in mice the concentration of Cu^{2+} ions in blood should preferably be ≤ 20 μg / mL to avoid aggregation of serum proteins.

***In vitro* stability of $CuCl_2$ in Mouse Serum**

The negligible tendency of $CuCl_2$ to induce protein aggregation at a concentration ≤ 20 μg / mL was corroborated by analysis of the dispersion behavior of the mouse serum medium over a prolonged period of 24 h (**Figure 4A**). Homogenous solution of $CuCl_2$ in mouse serum (20 μg / mL) displayed a near constant relaxation time of 2200 ms over a period of 24 h, confirming the stability of the suspension.

The stability of $^{64}CuCl_2$ at a concentration ≤ 20 μg / mL was further confirmed by radio-TLC assay. As indicated from the radio-TLC pattern (inset of **Figure 4B**), ^{64}Cu remained in ionic form ($^{64}Cu^{2+}$) in mouse serum medium over a period of 24 h. Thus it could be confirmed that $^{64}CuCl_2$ at a concentration ≤ 20 μg Cu / mL did not lead to aggregation of serum proteins incorporating ^{64}Cu over a prolonged period of 24 h.

Biodistribution Studies in Tumor Bearing Mice

The uptake of $^{64}CuCl_2$ produced by (n, γ) route in different organs/tissues of C57/BL6 mice bearing melanoma tumors and Swiss mice bearing fibrosarcoma tumors expressed as %ID/g at different p.i. times is shown in **Figures 5A** and **6A**. The results of the biodistribution studies revealed significant uptake of $^{64}CuCl_2$ in both melanoma as well fibrosarcoma tumors. In mice bearing melanoma tumors, tumor uptake of 5.8 ± 1.1 % ID/g was observed within 1 h p.i., which increased to 7.6 ± 1.7 %ID/g at 4 h p.i.. The uptake in fibrosarcoma tumor was slightly lower, wherein a maximum tumor uptake of 6.5 ± 1.4 %ID/g was observed at 4 h p.i.. For both melanoma and fibrosarcoma tumor bearing mice, initial accumulation of activity was observed in various non-target organs viz. liver, GIT, stomach, lungs etc. However, with the progress of time, the uptake in non-target organs gradually reduced. The tumor-to-blood, tumor-to-muscle and tumor-to-liver ratios of $^{64}CuCl_2$ at different time points p.i. are shown in **Figures 5B** and **6B**. In melanoma tumor bearing mice, the tumor-to-muscle ratio was observed to increase from 12.7 ± 1.2 at 1 h p.i. to 24.9 ± 1.8 at 24 h p.i., while the tumor-to-liver and tumor-to-blood ratios increased from 0.12 ± 0.07 to 0.62 ± 0.23 and 2.92 ± 0.65 to 13.27 ± 1.98, respectively, between the same time points. Similarly, in fibrosarcoma tumor bearing mice, the tumor-to-muscle, tumor-to-liver ratio and tumor-to-blood ratios were observed to increase from 10.11 ± 2.22 to

21.63 ± 1.77, 0.09 ± 0.04 to 0.75 ± 0.43, 2.05 ± 0.63 to 18.41 ± 1.68, respectively, between 1 h to 24 h p.i..

As a control experiment, ^{64}Cu-NOTA complex was administered in fibrosarcoma and melanoma tumor bearing mice and biodistribution studies were carried out at 4 h p.i. Since, maximum tumor uptake on administration of $^{64}CuCl_2$ was observed at 4 h p.i. in both the tumor models, this time point was chosen for the control studies. The uptake of ^{64}Cu-NOTA in different organs/tissues of C57/BL6 mice bearing melanoma tumors and fibrosarcoma tumors at 4 h p.i. times is shown in **Figure 7**. The figure also provides a comparison of uptakes of ^{64}Cu-NOTA and $^{64}CuCl_2$ in same animal models at 4 h p.i.. Uptakes of negatively charged ^{64}Cu-NOTA complex [21] in melanoma and fibrosarcoma tumors at 4 h p.i. were 0.12 ± 0.11 %ID/g and 0.09 ± 0.08 %ID/g, respectively, which are negligible compared to uptake of free $^{64}CuCl_2$ (as positively charged Cu^{2+} ions) in the same tumor models (**Figure 7**). As expected, ^{64}Cu-NOTA complex administered in mice rapidly cleared through renal route.

In order to validate that the biological efficacy of low specific activity $^{64}CuCl_2$ produced by (n, γ) route in a research reactor is comparable to that of NCA $^{64}CuCl_2$ produced by standard method in a cyclotron, the results of the biodistribution studies carried out in mice bearing melanoma tumors were compared with the results reported by Qin et al. (**Figure 8**). [14] In the reported method, biodistribution studies were carried out using NCA $^{64}CuCl_2$ in the same animal model. [14] The biodistribution patterns were compared at 4 h p.i. since the tumor uptake was highest at this time point. It can be seen from **Figure 8** that the biodistribution pattern of low specific activity $^{64}CuCl_2$ produced by (n, γ) route is comparable to that of NCA $^{64}CuCl_2$. The radioactivity cleared from the biological system through both hepatobiliary as well as renal route.

These results amply demonstrate the suitability of $^{64}CuCl_2$ produced by (n, γ) route as a radiotracer for PET imaging.

DISCUSSION

Copper is an essential micronutrient which plays a vital role in a variety of biochemical processes, which include cell proliferation, angiogenesis and tumor growth.[7, 14, 22] Over the last few years, several studies have explored copper metabolism as an imaging biomarker and increased copper uptake was observed in various types of cancerous tissues.[22] The increased uptake of copper ions in cancerous lesions could be attributed to human copper transporter 1 (CTR1), a 190-amino-acid protein of 28 kDa with 3 transmembrane domains.[12, 14] In fact, CTR1 is the primary protein responsible for copper transport in mammalian cells.[14] This protein is found to be overexpressed in a variety of cancer cells, and $^{64}CuCl_2$ has been used as a probe for non-invasive PET imaging of various types of tumor xenografts in preclinical studies.[11, 12, 14, 22] Such results hold tremendous promise as they provide evidence of the potential utility of simple injection of $^{64}Cu^{2+}$ ions for non-invasive visualization of tumors. Direct utilization of $^{64}CuCl_2$ would be much cheaper than the conventionally used PET probes involving complex targeting ligands and can easily be prepared while adhering to strict regulatory guidelines.

This strategy of direct utilization of neutron activated $^{64}CuCl_2$ as a PET radiotracer would especially be advantageous for countries with limited cyclotron facilities for radioisotope production. The International Atomic Energy Agency (IAEA) database provides a summary of approximately 251 research reactors currently operate worldwide. [10] Fifty of these research reactors have thermal neutron flux > 1×10^{14} $n.cm^{-2}.s^{-1}$, and the thermal flux of an additional 85 reactors ranges from 1×10^{12} - 1×10^{14} $n.cm^{-2}.s^{-1}$. Seventy eight of the above reactors are already

involved in radioisotope production, and these reactors have a good geographic distribution. Many of these research reactors can be used for production of neutron activated ^{64}Cu, which in turn would increase the global availability of this radioisotope.

Considering the cost of the target material for ^{64}Cu production, it can be expected that use of neutron activated ^{64}Cu would be much more cost-effective for clinical PET imaging studies where $^{64}CuCl_2$ can directly be used as a radiotracer. It is reported that when ^{64}Cu is produced by ^{64}Ni (p, n) ^{64}Cu reaction in a cyclotron, ~ 55 mg of enriched (> 95 %) ^{64}Ni target is required to produce ~ 22.2 GBq (600 mCi) of ^{64}Cu.[6] The cost of 1 g of enriched (> 95 %) ^{64}Ni target is ~ $ 32, 000. [23] Therefore, based on the cost of target material, the estimated cost of ~ 37 GBq (1 Ci) of ^{64}Cu produced in a cyclotron is ~ $ 3200. For countries with limited cyclotron facilities and which have to depend on imported ^{64}Cu to meet their research and clinical needs, the real cost of ^{64}Cu would be much higher if the decay loss of the radioactivity during transit is taken into consideration. On the contrary, adopting our method, ^{64}Cu can be produced by neutron activation of natural CuO target which is much cheaper (~ $ 600 for 1 g CuO). [24] The specific activity of neutron activated ^{64}Cu is ~ 3 TBq (80 Ci)/g. Based on similar considerations, the cost of ~ 37 GBq (1 Ci) of ^{64}Cu produced by neutron activation route in a medium flux research reactor is < $ 10. Thus, neutron activation route for production of ^{64}Cu is especially advantageous for routine clinical use in developing countries which have operational research reactors for radioisotope production.

It is pertinent to point out that much lower specific activity of neutron activated ^{64}Cu (~ 3 TBq / g) compared to that of NCA ^{64}Cu (3700 - 11,100 TBq / g) [6] might appear as a cause of concern especially when administered in human subjects in an uncomplexed form. It is well known that excess Cu is potentially hazardous to human health since it can participate in the

Fenton reaction, producing radical species which can lead to oxidative stress and subsequent oxidative damage to proteins, lipids and nucleic acids in the biological system. [25-27] However, for PET imaging in human subjects with good contrast, only 185-259 MBq (5-7 mCi) of $^{64}CuCl_2$ is expected to be administered.[28] Even while considering specific activity of ^{64}Cu as low as 740 MBq (20 mCi)/mg due to decay losses during transportation of the radioisotope to distant user sites, the radioactive solution would not contain > 0.5 mg Cu ions. It is reported that the cytotoxic effects of Cu ions are manifested at concentration ≥ 7.42 mg/L.[29, 30] Assuming that the volume of volume of blood in an average adult varies between 4-5 L, the concentration of Cu^{2+} ions in human blood when administered for PET imaging would be much lower than the cytotoxic limit. However, for therapeutic procedures wherein larger doses need to be administered, detailed dosimetry and toxicity studies would be required before human administration.

Another important issue concerning the use of low specific activity $^{64}CuCl_2$ as an imaging probe is the possibility of aggregation of serum proteins in presence of Cu^{2+} ions.[19] In case there is an aggregation of serum protein incorporating ^{64}Cu after *in vivo* administration of $^{64}CuCl_2$, a high uptake of the radioactivity would be observed in reticuloendothelial system (RES). The radioactivity incorporated protein aggregates would rapidly be cleared through the hepatobiliary route and negligible tumor uptake would be observed. The aggregation of serum proteins in presence of Cu^{2+} ions was not of much concern in the earlier studies with cyclotron produced NCA $^{64}CuCl_2$[14, 22] wherein the concentration of Cu^{2+} ions administered *in vivo* was extremely low. In order to investigate the possibility of aggregation of serum proteins on administration of low specific activity $^{64}CuCl_2$ in biological system, DLS studies after addition of different concentrations of non-radioactive $CuCl_2$ in serum medium were carried out. The results

of these studies indicated that aggregate formation would be manifested only at a concentration > 20 µg Cu / mL of serum. Since a healthy mouse generally has ~ 1 mL of blood, a maximum amount of 20 µg of Cu corresponding to 14.8 MBq (0.4 mCi) of ^{64}Cu (assuming specific activity as low as 740 MBq (20 mCi)/mg due to decay losses) can be administered which is adequate for small animal PET imaging.[31, 32] Based on similar considerations, administration of ~ 185 MBq (5 mCi) $^{64}CuCl_2$ which is adequate for PET imaging in human subjects [28] would not result in aggregation of serum proteins *in vivo*. Thus, low specific activity $^{64}CuCl_2$ produced through (n, γ) route in nuclear reactors can safely be used as a PET probe in clinical studies.

Ex vivo biodistribution studies after administration of $^{64}CuCl_2$ in tumor bearing mice showed that the radiotracer accumulated in the tumor rapidly and a decent tumor-to-background contrast could be achieved with 4 h p.i.. Negligible tumor uptake of negatively charged ^{64}Cu-NOTA complex along with rapid clearance of the radioactivity through renal route validated that the increased tumor uptake of $^{64}CuCl_2$ was indeed due to cellular uptake of free $^{64}Cu^{2+}$ ions. Though *in vivo* PET imaging could not be carried out due to unavailability of small animal PET imaging facility in our research centre, the results of this study amply demonstrated that neutron activated $^{64}CuCl_2$ is an effective PET probe for non-invasive detection of various types of cancers. The only limitation of this radiotracer is that it might not be suitable for detection of primary cancer or its metastasis in the abdominal region because of the excretion of most $^{64}CuCl_2$ from the liver to the intestinal tract through the bile ducts. [14] The biodistribution pattern observed after administration of neutron activated $^{64}CuCl_2$ in tumor bearing mice was comparable to that with NCA $^{64}CuCl_2$. [14] It is envisaged that the promising results obtained in this study would set the stage for widespread utilization of neutron activated $^{64}CuCl_2$ in clinical context.

CONCLUSIONS

In this study, we established the feasibility of using low specific activity $^{64}CuCl_2$ produced by (n, γ) route, as a cost-effective radiotracer for non-invasive visualization of tumors by PET. A viable strategy for large-scale production of ^{64}Cu with high radionuclidic purity and acceptable specific activity for use as a PET radiotracer was developed by careful optimization of irradiation parameters. *In vitro* studies revealed that $^{64}CuCl_2$ remains in ionic form in the biological system at doses suitable for PET imaging in both preclinical as well as clinical settings. Biodistribution studies carried out in mice bearing melanoma and fibrosarcoma tumors revealed rapid and significant tumor uptake with a satisfactory tumor-to-background ratio achieved within 4 h p.i. of $^{64}CuCl_2$. The practicality of low specific activity $^{64}CuCl_2$ as a PET radiotracer was found to be comparable to its NCA counterpart in terms of tumor targeting efficacy and pharmacokinetic profile, which demonstrated the enormous potential of neutron activated ^{64}Cu to become the radionuclide of choice for future PET procedures, especially in countries with limited cyclotron facilities.

ACKNOWLEDGEMENTS

Research at Bhabha Atomic Research Centre is a part of ongoing activities of the Department of Atomic Energy, India and is fully supported by government funding. The authors are grateful to Dr. K. L. Ramakumar, Director, Radiochemistry and Isotope Group, Bhabha Atomic Research Centre for his valuable support to this program. Thanks are due to Mr. K. C. Jagadeesan and Dr. S. V. Thakare for arranging the irradiation of the CuO targets in the Dhruva reactor of our research centre.

Figure captions:

Figure 1: Production of neutron activated ^{64}Cu. (A) Production of ^{64}Cu along and possibility of co-production of radionuclidic impurities on irradiation of natural CuO target in a research reactor. (B) γ-spectra of ^{64}Cu (i) just after completion of radiochemical processing and (ii) after decay for 7 days.

Figure 2: Optimization of irradiation conditions for production of neutron activated ^{64}Cu based on theoretical calculations using Bateman equation. (A) Specific activity of ^{64}Cu, (b) Level of ^{65}Zn impurity co-produced (as a % of ^{64}Cu), on irradiation of 1.25 g CuO (equivalent to 1 g Cu) target at different flux positions for different time intervals.

Figure 3: Correlation function from serum samples containing (A) Different concentration of $CuCl_2$, (B) 26.7 μg Cu / mL of serum at different time intervals. Inset shows the variation in effective particle size of serum sample with time.

Figure 4: Stability of $CuCl_2$ in serum medium. (A) Measurement of relaxation time over a period of 24 h. (B) Percentage of $^{64}CuCl_2$ as free $^{64}Cu^{2+}$ ions in serum medium over a period of 24 h. Inset shows the TLC pattern of $^{64}CuCl_2$ in serum medium when developed in 0.1 M sodium citrate solution.

Figure 5: Biodistribution of $^{64}CuCl_2$ in C57BL/6 mice bearing melanoma tumors. (A) Uptake of $^{64}CuCl_2$ in different organs/tissues at different time points p.i.. (B) The tumor-to-blood, tumor-to-muscle and tumor-to-liver ratios of $^{64}CuCl_2$ at different time points p.i..

Figure 6: Biodistribution of $^{64}CuCl_2$ in Swiss mice bearing fibrosarcoma tumors. (A) Uptake of $^{64}CuCl_2$ in different organs/tissues at different time points p.i.. (B) The tumor-to-blood, tumor-to-muscle and tumor-to-liver ratios of $^{64}CuCl_2$ at different time points p.i..

Figure 7: Comparison of biodistribution patterns of ^{64}Cu-NOTA and $^{64}CuCl_2$ at 4 h p.i. in (A) C57BL/6 mice bearing melanoma tumors, (B) Swiss mice bearing fibrosarcoma tumors.

Figure 8: Comparison of biodistribution patterns of neutron activated $^{64}CuCl_2$ and NCA $^{64}CuCl_2$ at 4 h p.i. in C57BL/6 mice bearing melanoma tumors.

Table 1: Production of (n,γ)^{64}Cu in different batches by irradiation of natural CuO target in the Dhruva reactor at a flux of ~ 1 × 10^{14} n.cm^{-2}.s^{-1} for 7 days

Batch No.	Target weight (mg)	At the end of radiochemical processing *(8 h after end of irradiation)*			After decay for 24 h *(16 h after end of radiochemical processing)*		
		Activity of ^{64}Cu [GBq (Ci)]	Specific activity of ^{64}Cu [TBq (Ci)/g]	^{65}Zn impurity in ^{64}Cu (%)	Activity of ^{64}Cu [GBq (Ci)]	Specific activity of ^{64}Cu [TBq (Ci)/g]	^{65}Zn impurity in ^{64}Cu (%)
1	13.3	30.7 (0.83)	2.9 (78.3)	1.8×10^{-6}	13.0 (0.35)	1.2 (33.0)	4.3×10^{-6}
2	15.0	35.5 (0.96)	3.0 (80.6)	2.4×10^{-6}	15.0 (0.40)	1.3 (33.6)	5.4×10^{-6}
3	22.1	56.6 (1.53)	3.2 (86.9)	1.2×10^{-6}	23.9 (0.64)	1.3 (36.3)	2.9×10^{-6}
4	14.2	36.5 (0.99)	3.1 (83.2)	2.1×10^{-6}	15.5 (0.42)	1.3 (35.3)	5.1×10^{-6}
5	13.0	34.0 (0.91)	3.2 (87.8)	1.3×10^{-6}	14.3 (0.38)	1.4 (36.6)	3.1×10^{-6}

References

1. M. D. Farwell, A. S. Clark and D. A. Mankoff, *JAMA Oncol*, 2015, **1**, 421-2.
2. A. Mahajan, V. Goh, S. Basu, R. Vaish, A. J. Weeks, M. H. Thakur and G. J. Cook, *Clin Radiol*, 2015 (In press).
3. G. C. Pereira, M. Traughber and R. F. Muzic, Jr., *Biomed Res Int*, 2014, **2014**, 231090.
4. R. Weissleder and M. J. Pittet, *Nature*, 2008, **452**, 580-9.
5. S. M. Ametamey, M. Honer and P. A. Schubiger, *Chem Rev*, 2008, **108**, 1501-16.
6. D. W. McCarthy, R. E. Shefer, R. E. Klinkowstein, L. A. Bass, W. H. Margeneau, C. S. Cutler, C. J. Anderson and M. J. Welch, *Nucl Med Biol*, 1997, **24**, 35-43.
7. A. Niccoli Asabella, G. L. Cascini, C. Altini, D. Paparella, A. Notaristefano and G. Rubini, *Biomed Res Int*, 2014, **2014**, 786463.
8. T. Bokhari, A. Mushtaq and I. Khan, *J Radioanal Nucl Chem*, 2010, **284**, 265-71.
9. K. V. Vimalnath, A. Rajeswari, V. Chirayil, P. L. Sharad, K. C. Jagadeesan, P. V. Joshi and M. Venkatesh, *J Radioanal Nucl Chem*, 2011, **290**, 221-5.
10. *International Atomic Energy Agency. Operation Research Reactors in the World [database]. Available at: www.naweb.iaea.org/napc/physics/research_reactors/database/RR%20Data%20Base/datasets/foreword_home.html.*
11. K. I. Kim, S. J. Jang, J. H. Park, Y. J. Lee, T. S. Lee, K. S. Woo, H. Park, J. G. Choe, G. I. An and J. H. Kang, *J Nucl Med*, 2014, **55**, 1692-8.
12. F. Peng, X. Lu, J. Janisse, O. Muzik and A. F. Shields, *J Nucl Med*, 2006, **47**, 1649-52.
13. F. Peng, O. Muzik, J. Gatson, S. G. Kernie and R. Diaz-Arrastia, *J Nucl Med*, 2015, **56**, 1252-7.

14. C. Qin, H. Liu, K. Chen, X. Hu, X. Ma, X. Lan, Y. Zhang and Z. Cheng, *J Nucl Med*, 2014, **55**, 812-7.

15. R. Chakravarty, S. Chakraborty, A. Dash, M.R.A. Pillai, *Nucl. Med. Biol.* 2013, **40**, 197-205.

16. Y. Zhang, H. Hong, J. W. Engle, J. Bean, Y. Yang, B. R. Leigh, T. E. Barnhart and W. Cai, *PLoS One*, 2011, **6**, e28005.

17. D. P. Fairhurst, S. Prescott, *Spectrosc. Eur.*, 2011, **23**, 13-6.

18. J. Cetnar, *Annals Nucl Energy*, 2006, **33**, 640-45.

19. W. Bal, M. Sokołowska, E. Kurowska, P. Faller. *Biochim Biophys Acta*, 2013, **1830**, 5444-55.

20. P. A. Hassan, S. Rana and G. Verma, *Langmuir*, 2015, **31**, 3-12.

21. R. Ferdania, D. J. Stigersb, A. L. Fiamengoa, L. Weia, B. T. Y. Lib, J. A. Golenc, A. L. Rheingoldd, G. R. Weismanb, E. H. Wong, C. J. Anderson. *Dalton Trans,* 2012, **41**, 1938–1950.

22. A. Duatti, *Nucl Med Biol*, 2015, **42**, 215-8.

23. Isoflex product catalog (http://www.isoflex.com/nickel-64). Accessed on September 28, 2015.

24. Sigma-Aldrich product catalog. (http://www.sigmaaldrich.com/catalog/product/aldrich/450812?lang=en&region=IN). Accessed on September 28, 2015.

25. J. Y. Uriu-Adams and C. L. Keen, *Mol Aspects Med*, 2005, **26**, 268-98.

26. M. Valko, C. J. Rhodes, J. Moncol, M. Izakovic and M. Mazur, *Chem Biol Interact*, 2006, **160**, 1-40.

27. A. Gupte and R. J. Mumper, *Cancer Treat Rev*, 2009, **35**, 32-46.

28. A. Pfeifer, U. Knigge, T. Binderup, J. Mortensen, P. Oturai, A. Loft, A. K. Berthelsen, S. W. Langer, P. Rasmussen, D. Elema, E. von Benzon, L. Hojgaard and A. Kjaer, *J Nucl Med*, 2015, **56**, 847-54.

29. C. A. Grillo, M. A. Reigosa and M. A. de Mele, *Contraception*, 2010, **81**, 343-9.

30. C. A. Grillo, M. A. Reigosa and M. F. Lorenzo de Mele, *Mutat Res*, 2009, **672**, 45-50.

31. R. Chakravarty, S. Goel, H. Hong, F. Chen, H. F. Valdovinos, R. Hernandez, T. E. Barnhart and W. Cai, *Nanomedicine (Lond)*, 2015, **10**, 1233-46.

32. R. Hernandez, A. Czerwinski, R. Chakravarty, S. A. Graves, Y. Yang, C. G. England, R. J. Nickles, F. Valenzuela and W. Cai, *Eur J Nucl Med Mol Imaging*, 2015 (In press).

$^{64}CuCl_2$ Produced by Direct Neutron Activation Route as a Cost-Effective Probe for Cancer Imaging: The Journey has Begun

Rubel Chakravarty,[1,,#] Sudipta Chakraborty,[1,#] K. V. Vimalnath,[1] Priyalata Shetty,[1] Haladhar Dev Sarma,[2] P. A. Hassan[3] and Ashutosh Dash[1,*]*

[1]Isotope Production and Applications Division, [2]Radiation Biology and Health Sciences Division, [3]Chemistry Division, Bhabha Atomic Research Centre, Trombay, Mumbai 400 085, India

Graphical Abstract

Neutron activated $^{64}CuCl_2$ is a cost-effective PET probe for non-invasive visualization of various types of cancers.

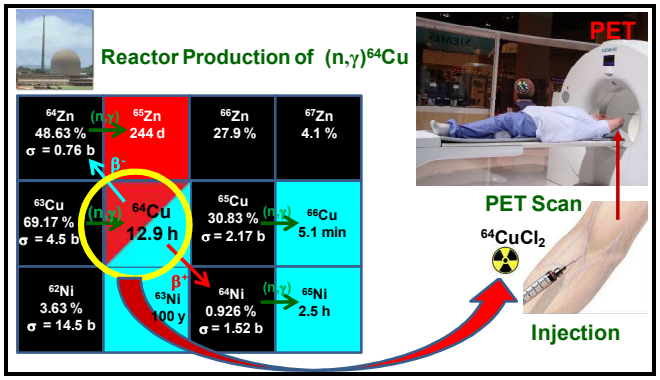

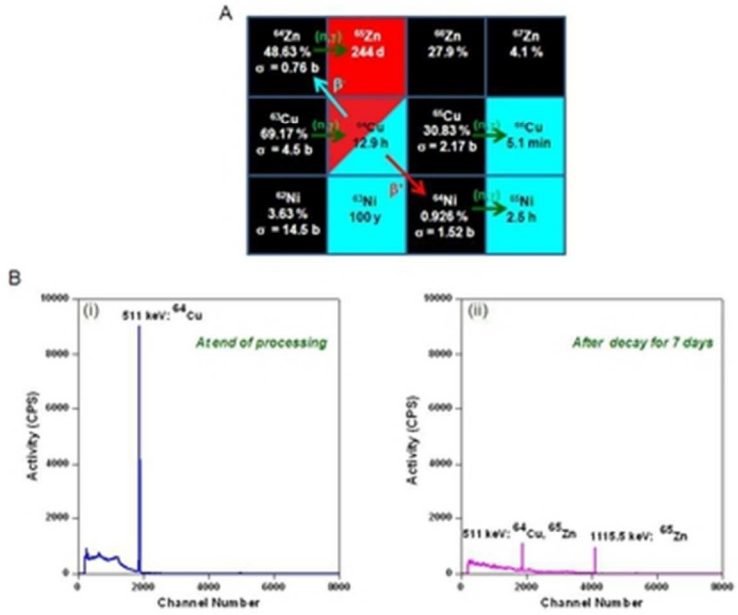

Figure 1: Production of neutron activated 64Cu. (A) Production of 64Cu along and possibility of co-production of radionuclidic impurities on irradiation of natural CuO target in a research reactor. (B) γ-spectra of 64Cu (i) just after completion of radiochemical processing and (ii) after decay for 7 days.
33x27mm (300 x 300 DPI)

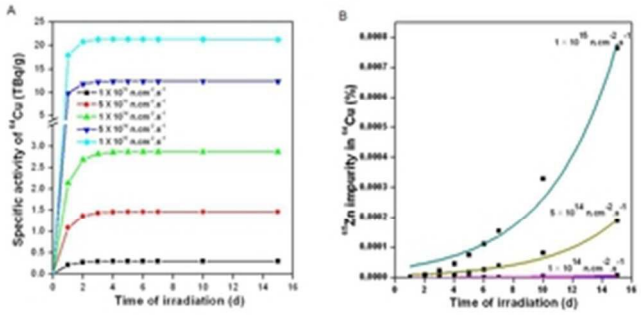

Figure 2: Optimization of irradiation conditions for production of neutron activated 64Cu based on theoretical calculations using Bateman equation. (A) Specific activity of 64Cu, (b) Level of 65Zn impurity co-produced (as a % of 64Cu), on irradiation of 1.25 g CuO (equivalent to 1 g Cu) target at different flux positions for different time intervals.
29x15mm (300 x 300 DPI)

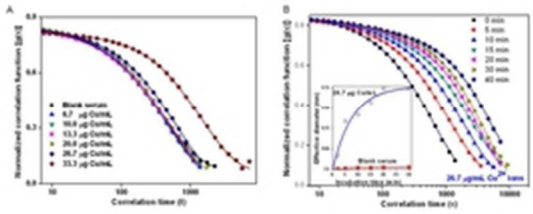

Figure 3: Correlation function from serum samples containing (A) Different concentration of CuCl2, (B) 26.7 µg Cu / mL of serum at different time intervals. Inset shows the variation in effective particle size of serum sample with time.
24x9mm (300 x 300 DPI)

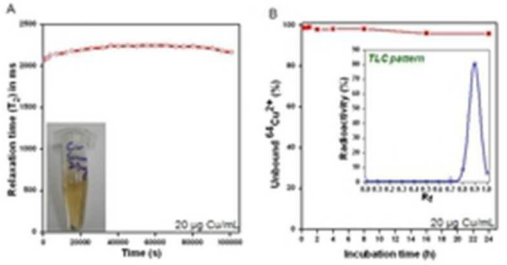

Figure 4: Stability of CuCl2 in serum medium. (A) Measurement of relaxation time over a period of 24 h. (B) Percentage of 64CuCl2 as free 64Cu2+ ions in serum medium over a period of 24 h. Inset shows the TLC pattern of 64CuCl2 in serum medium when developed in 0.1 M sodium citrate solution.
23x12mm (300 x 300 DPI)

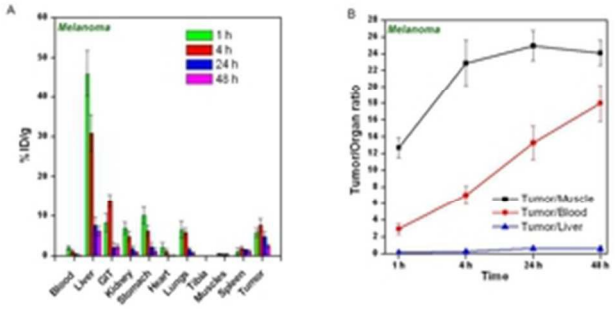

Figure 5: Biodistribution of 64CuCl2 in C57BL/6 mice bearing melanoma tumors. (A) Uptake of 64CuCl2 in different organs/tissues at different time points p.i.. (B) The tumor-to-blood, tumor-to-muscle and tumor-to-liver ratios of 64CuCl2 at different time points p.i..
27x14mm (300 x 300 DPI)

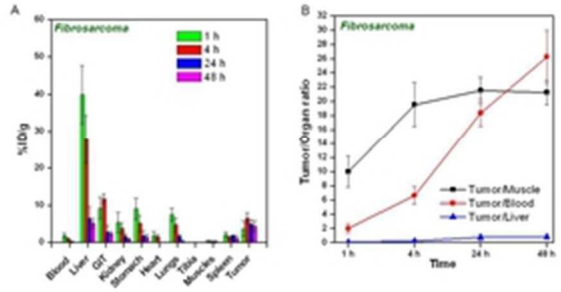

Figure 6: Biodistribution of 64CuCl2 in Swiss mice bearing fibrosarcoma tumors. (A) Uptake of 64CuCl2 in different organs/tissues at different time points p.i.. (B) The tumor-to-blood, tumor-to-muscle and tumor-to-liver ratios of 64CuCl2 at different time points p.i..
25x13mm (300 x 300 DPI)

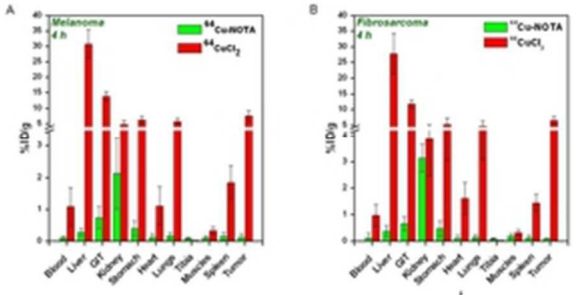

Figure 7: Comparison of biodistribution patterns of 64Cu-NOTA and 64CuCl2 at 4 h p.i. in (A) C57BL/6 mice bearing melanoma tumors, (B) Swiss mice bearing fibrosarcoma tumors.
26x13mm (300 x 300 DPI)

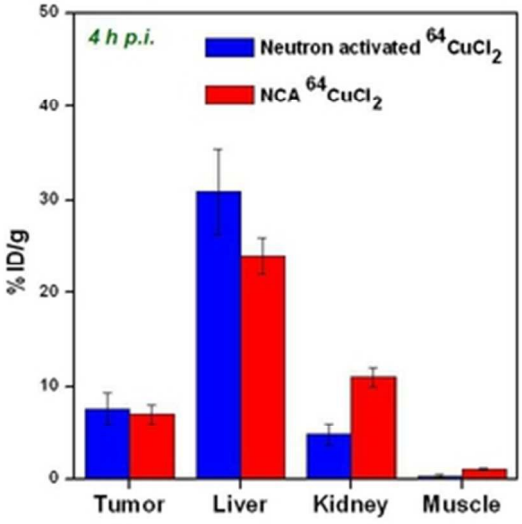

Figure 8: Comparison of biodistribution patterns of neutron activated 64CuCl2 and NCA 64CuCl2 at 4 h p.i. in C57BL/6 mice bearing melanoma tumors.
27x27mm (300 x 300 DPI)